Neurobiology of Disease

Early TNF-Dependent Regulation of Excitatory and Inhibitory Synapses on Striatal Direct Pathway Medium Spiny Neurons in the YAC128 Mouse Model of Huntington's Disease

Julien Chambon, Pragya Komal, Gil M. Lewitus, Gina M. Kemp, Simone Valade, Houaria Adaïdi, Noura Al Bistami, and David Stellwagen

Department of Neurology and Neurosurgery, Centre for Research in Neuroscience, Research Institute of the McGill University Health Center, Montréal, Québec H3G 1A4, Canada

Huntington's disease (HD) is a neurodegenerative disease caused by a polyglutamine expansion in the huntingtin gene. Neurodegeneration first occurs in the striatum, accompanied by an elevation in inflammatory cytokines. Using the presymptomatic male YAC128 HD model mouse, we examined the synaptic input onto the striatal medium spiny neurons to look for early changes that precede degeneration. We observed an increase in excitatory synaptic strength, as measured by AMPA/NMDA ratios, specifically on direct pathway D1 receptor expressing medium spiny neurons, with no changes on indirect pathway neurons. The changes in excitation were accompanied by a decrease in inhibitory synaptic strength, as measured by the amplitude of miniature inhibitory synaptic currents. The pro-inflammatory cytokine tumor necrosis factor alpha (TNF) was elevated in the striatum of YAC128 at the ages examined. Critically, the changes in excitatory and inhibitory inputs are both dependent on TNF signaling, as blocking TNF signaling genetically or pharmacological normalized synaptic strength. The observed changes in synaptic function are similar to the changes seen in D1 medium spiny neurons treated with high levels of TNF, suggesting that saturating levels of TNF exist in the striatum even at early stages of HD. The increase in glutamatergic synaptic strength and decrease in inhibitory synaptic strength would increase direct pathway neuronal excitability, which may potentiate excitotoxicity during the progress of HD.

Key words: cytokine; Huntington's disease; inflammation; plasticity; striatum; TNF

Significance Statement

The striatum is the first structure to degenerate in Huntington's disease, but the early changes that presage the degeneration are not well defined. Here we identify early synaptic changes in the YAC128 mouse model of Huntington's disease specifically on a subpopulation of striatal neurons. These neurons have stronger excitatory synapses and weaker inhibitory inputs, and thus would increase the susceptibility to excitotoxicity. These changes are dependent on signaling by the pro-inflammatory cytokine TNFα. TNF is elevated even at early presymptomatic stages, and blocking TNF signaling even acutely will reverse the synaptic changes. This suggests early intervention could be important therapeutically.

Introduction

Huntington's disease (HD) is an incurable neurodegenerative disease caused by an autosomal dominant mutation in the huntingtin gene, resulting from a variable expansion of a CAG repeat encoding polyglutamine. Although the gene expansion was identified >20 years ago, the mechanistic details of the disease remain obscure. Despite ubiquitous expression of the mutant huntingtin protein (mHTT), neurodegeneration first occurs in the striatum both clinically and in mouse models of the disease (Bates et al., 2015). Further, HD motor symptoms generally precede cell death in the striatum, which is relatively late in patients (Caramins et al., 2003) and mouse models (Turmaine et al., 2000). This suggests that changes in striatal circuit function occur early in HD and may contribute to the later degeneration. Indeed, early changes in striatal development and circuitry can be observed
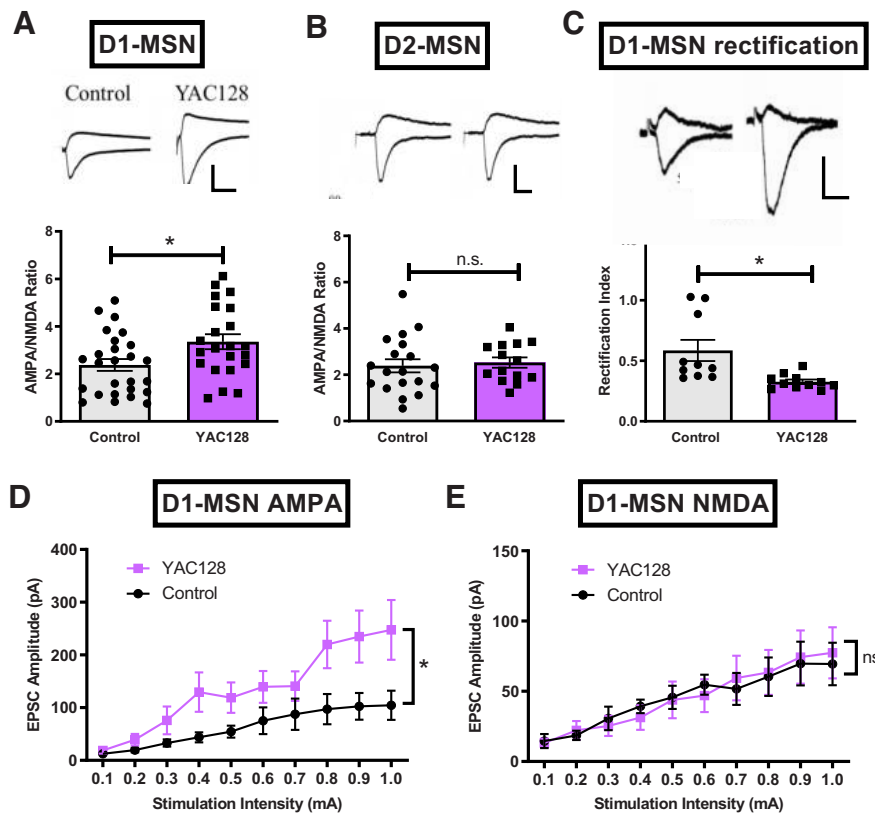
Figure 1. Increased glutamatergic synaptic strength on D1-MSNs in presymptomatic YAC128 mice. **A**, Sample traces and group data of the AMPA/NMDA ratio of dorsal striatal D1-MSNs from 8- to 12-week-old male mice carrying the YAC128 transgene, compared with nonexpressing littermates. The HD model mice has a significant increase in ratio (two-tailed t test, $t_{(46)} = 2.457$, $p = 0.0178$). Calibration: 100 pA, 20 ms. **B**, Sample traces and group data of AMPA/NMDA ratios for D2-MSNs from the same mice revealed no differences between YAC128 mice and control littermates (two-tailed t test, $t_{(31)} = 0.3686$, $p = 0.7149$). Calibration: 80 pA, 20 ms. **C**, Sample traces and group data of isolated AMPA current amplitudes at −70 and +40 mV, compared for degree of AMPAR rectification (as +40 current over −70 current). D1-MSNs from YAC128 mice have a larger rectification index, indicating a greater amount of rectification, than control littermates (t test with Welch's correction; Levene test, $p < 0.0001$; $t_{(9.780)} = 2.894$, $p = 0.0163$). Calibration: 50 pA, 20 ms. **D**, I/O curves of AMPAR currents on D1-MSN demonstrate larger AMPA currents across the stimulation intensities for YAC128 mice compared with control littermates (two-way repeated-measures ANOVA, $F_{(1,12)} = 8.466$; main effect of genotype, $p = 0.0131$). **E**, I/O curves of NMDAR currents were not different on D1-MSNs between YAC128-expressing mice and control littermates (two-way repeated-measures ANOVA, $F_{(1,8)} = 0.0002862$, $p = 0.9869$).

in pre-HD children as young as 10 years old (van der Plas et al., 2019; Tereshchenko et al., 2020).

The striatum, consisting of the caudate and putamen, is a major structure within the basal ganglia and has important roles in motor control; ∼90% of the striatum is composed of GABAergic medium spiny neurons (MSNs), which constitute the sole output of the striatum (Lanciego et al., 2012). MSNs receive excitatory input from the cortex, thalamus, amygdala, and hippocampus; inhibitory input from striatal interneurons as well as collaterals from neighboring MSNs; and cholinergic input from striatal interneurons (Lebouc et al., 2020). These neurons are further subcategorized depending on their receptor expression and target region. MSNs expressing the dopamine D1 receptors (D1-MSNs) are generally part of the direct pathway involved in the initiation of movements. The MSNs that express the dopamine D2 receptors (D2-MSNs) are usually part of the indirect pathway involved in the suppression of unwanted movements. There may also be differences between direct and indirect pathway MSNs in HD: D2-MSNs seem to be affected by neurodegeneration before D1-MSNs; however, D1-MSNs appear to have earlier changes in synaptic function (Raymond et al., 2011; Goodliffe et al.,

2018). Changes in glutamatergic inputs to the striatum precede the development of symptoms in mouse models and are detectable as early as 1 month of age (Raymond et al., 2011). Changes have also been observed in extrasynaptic receptors, particularly extrasynaptic NMDARs (Milnerwood et al., 2010). Further, GABAergic synapses also seem disrupted in HD. Expression of mHTT led to decreased number of GABA-A receptors at the neuronal surface and reduced inhibitory synaptic currents (Twelvetrees et al., 2010).

Inflammation, known to be associated with HD, is a potential mediator of the synaptic changes on MSNs. Inflammatory cytokines, including TNF, are increased in the striatum of both patients and mouse models of HD (Soulet and Cicchetti, 2011), although whether this occurs in presymptomatic animals is uncertain (Alto et al., 2014). Further, HD patients (including presymptomatic carriers) have elevated levels of TNF and IL6 in plasma and CSF (Bjorkqvist et al., 2008). This is intriguing as TNF can lead to changes in synaptic receptor content, although this can be bidirectional (Heir and Stellwagen, 2020). TNF can lead to the exocytosis of AMPARs in cortical and hippocampal pyramidal cells (Beattie et al., 2002), but to the preferential endocytosis of AMPARs on MSNs (Lewitus et al., 2014).

Therefore, we wanted to investigate whether TNF has a role in HD development by looking for TNF-dependent changes in MSN synapses in a presymptomatic mouse model. We used a common HD model, the YAC128 mouse, which expresses the full-length human HTT with 128 CAG repeats in a yeast artificial chromosome (Hodgson et al., 1999; Slow et al., 2003). This mouse model is a well-studied HD model with good validity (Pouladi et al., 2013), and exhibits motor deficits by 3 months of age, and cortical neuronal loss at ∼9 months of age. Here we looked at the presymptomatic mouse, at 8-12 weeks of age, and observed TNF-dependent changes at both glutamatergic and GABAergic synapses.

Materials and Methods
Animals
All mutant lines were acquired from The Jackson Laboratory. YAC128 mice (Hodgson et al., 1999; Slow et al., 2003) (FVB-Tg(YAC128)53Hay/J; RRID:IMSR_JAX:004938) were bred with both TNF$^{-/-}$ mice on a C57Bl6/J background (B6.129S-TNF(tm1Gkl)/J; RRID:IMSR_JAX:005540) and mice expressing the tD-Tomato fluorescent protein under the dopamine D1 receptor promoter (B6Cg-Tg(Drd1a-tdTomato)6Calak/J; RRID: IMSR_JAX:016204). Mice were bred for ≥6 generations on the C57Bl6/J background. Both the D1-tdTomato and YAC128 were kept hemizygously. Only male mice 8-12 weeks of age were used for all biochemical and electrophysiological experiments, with YAC128-expressing mice compared with non–YAC128-expressing littermates. HD-like disease progression is slightly different in male and female mice, with earlier locomotor changes in males

(Menalled et al., 2009); we therefore used males to test for early changes. TNFR1$^{-/-}$ mice (C57BL/6-Tnfrsf1a(tm1Imx)/J; RRID:IMSR_JAX:003242) were maintained homozygously. All animal procedures were performed in accordance with the guidelines of the Canadian Council for Animal Care and the Montreal General Hospital Animal Facility Care Committee.

Drug treatments

The dominant-negative (DN) TNF (XENP1595, Xencor Biotherapeutics) was injected subcutaneously, 48 h before experiments, at a concentration of 30 mg/kg. Acute slices were incubated in 10-1000 ng/ml recombinant mouse TNF (Genscript, catalog #Z03333) in ACSF for 30 min at 30°C.

Electrophysiology

Acute slice preparation and recording. Mouse brains were dissected and placed in an oxygenated, ice-cold solution containing the following (in mM): 92 choline chloride, 2.5 KCl, 1.2 NaH$_2$PO$_4$, 30 NaHCO$_3$, 20 HEPES, 25 glucose, 5 sodium ascorbate, 3 sodium pyruvate, 10 MgSO$_4$, 0.5 CaCl$_2$ (300-310 mOsm, pH 7.3). The brains were then sliced using a vibratome (Leica VT1200) to obtain 300-μm-thick coronal slices containing the dorsal striatum. For recording, slices were perfused with ACSF, containing the following (in mM): 119 NaCl, 2.5 KCl, 1 NaH$_2$PO$_4$, 1.3 MgCl$_2$, 2.5 CaCl$_2$, 26.2 NaHCO$_3$, 11 glucose (290 mOsm and pH 7.3), saturated with 95% O$_2$/5% CO$_2$ and perfused at 30°C at 1.5-2 ml/min. Whole-cell voltage-clamp recordings were acquired using an Axopatch 200B (Molecular Devices), filtered at 2 kHz and digitized at 10 kHz, using a Digidata 1440A (Molecular Devices). All signals were recorded using Clampex 10.6 (Molecular Devices). The series resistance was ~25-30 MΩ and was not compensated. D1-MSNs were identified using fluorescence and morphologic differences, D2-MSNs by morphology and lack of fluorescence.

AMPA/NMDA ratios, rectification index, and I/O curves. EPSCs were evoked using a stainless-steel bipolar electrode, placed under the cortex in the white matter, close to the recorded neuron. Whole-cell glass electrodes (3-6 MΩ tips) were filled with excitatory internal solution containing the following (in mM): 122 cesium methane sulfonate, 8 NaCl, 10 glucose, 1 CaCl$_2$, 10 HEPES, 10 EGTA, 0.3 Na$_3$-GTP, 2 Mg-ATP (308-310 mOsm, pH 7.3). First, we recorded evoked synaptic responses at −70 mV to measure the AMPAR-mediated EPSCs. NMDAR-mediated EPSCs were recorded at +40 mV. Both recordings were performed in the presence of 100 μM picrotoxin to block GABA$_A$ receptor functions. AMPA/NMDA ratio was obtained as a ratio of peak AMPAR-mediated current (−70 mV), and the current 40 ms post-peak AMPAR-mediated current (+40 mV), to ensure a relatively pure NMDA response. The rectification index was calculated as a ratio of EPSC amplitudes between −70 and +40 mV, under NMDAR blockade, using peaks for both measures. For input-output (I/O) curves, cells were stimulated at a set range of stimulation intensity, using the previously described stimulating electrode. I/O recordings were done in the presence of either 50 μM NBQX to block AMPAR activity or 50 μM AP-5 to block NMDAR activity. All EPSCs used for analysis were averaged from 10 to 20 responses per condition.

mIPSCs. mIPSCs were recorded using the whole-cell glass electrodes filled with inhibitory internal solution containing the following (in mM): 127 CsCl, 8 NaCl, 10 glucose, 1 CaCl$_2$, 10 HEPES, 10 EGTA, 0.3 Na$_3$-GTP, 2 Mg-ATP (308-310 mOsm, pH 7.3). For each cell recorded, ~100 events were used to determine both the mIPSC amplitude and frequency. Recordings were done in the presence of 500 nM TTX and 50 μM NBQX to block voltage-gated sodium channels and AMPAR activity, respectively.
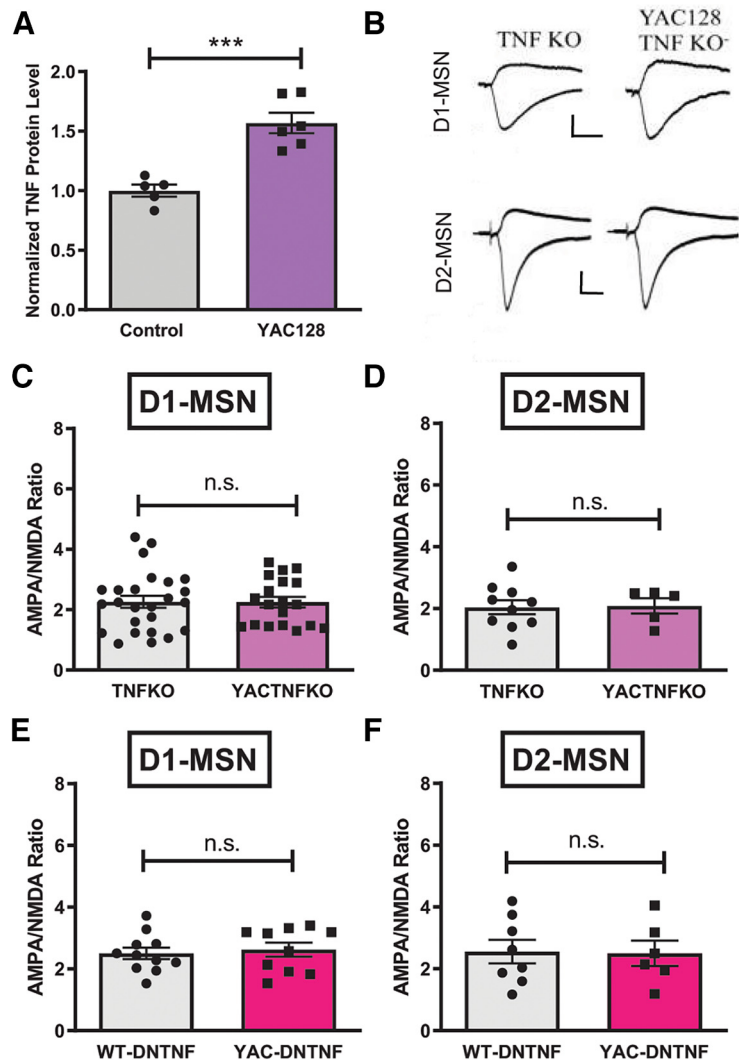

Figure 2. Increased glutamatergic synaptic strength in YAC128 mice is dependent on TNF signaling. ***A***, TNF levels are elevated in the striatum of 8- to 12-week-old YAC128 mice, as measured by a TNF ELISA, compared with control littermates (two-tailed *t* test, $t_{(9)} = 5.407$, $p = 0.0004$). ***B***, Sample traces of evoked EPSCs recorded at −70 and +40 mV, used to calculate AMPA/NMDA ratios, for D1-MSNs and D2-MSNs from $TNF^{-/-}$ mice and $TNF^{-/-}$; YAC128 mice. Calibration: 50 pA, 20 ms. ***C***, Group data showing that, in $TNF^{-/-}$ mice, YAC128 expression does not alter AMPA/NMDA ratios on D1-MSNs (two-tailed *t* test, $t_{(42)} = 0.03911$, $p = 0.9690$). ***D***, AMPA/NMDA ratios are also unchanged on D2-MSNs in $TNF^{-/-}$; YAC128 mice, compared with $TNF^{-/-}$ control littermates (two-tailed *t* test, $t_{(13)} = 0.1233$, $p = 0.9037$). ***E***, Treatment of YAC128 mice with DN-TNF (30 mg/kg; s.c.) 48 h before recording restored AMPA/NMDA ratios on D1-MSNs to levels comparable to DN-TNF-treated control littermates (two tailed *t* test, $t_{(19)} = 0.4109$, $p = 0.6857$). ***F***, The AMPA/NMDA ratios on D2-MSNs were unaffected by DN-TNF treatment for both YAC128 mice and their control littermates (two-tailed *t* test, $t_{(12)} = 0.09473$, $p = 0.9261$).

TNF ELISA

The TNF ELISA kit (BE69212, IBL) was performed according to the manufacturer's instructions. Briefly, the striatum was dissected and flash frozen. Tissue samples were then homogenized in 400 μl of PBS with a protease inhibitor cocktail (Bioshop Canada, PIC002.1), and protein content normalized using a BCA assay. Samples were then run on the ELISA kit, as per the kit protocol.

Surface biotinylation. Surface biotinylation was done as previously described (Lewitus et al., 2014). Briefly, striatal slices were treated with TNF (100 or 1000 ng/ml) for 45 min in ACSF, washed 3× with ice-cold ACSF, and incubated for 30 min with 1 mg/ml Sulfo-NHS-SS-Biotin (Thermo Scientific) diluted in ice-cold ACSF. Slices were then washed 3× with ice-cold ACSF containing 100 mM glycine and lysed in 1% Triton X-100, 0.1% SDS in PBS, with a protease inhibitor cocktail (Bioshop Canada, PIC002.1). Slices were homogenized in lysis buffer through a 28 gauge syringe
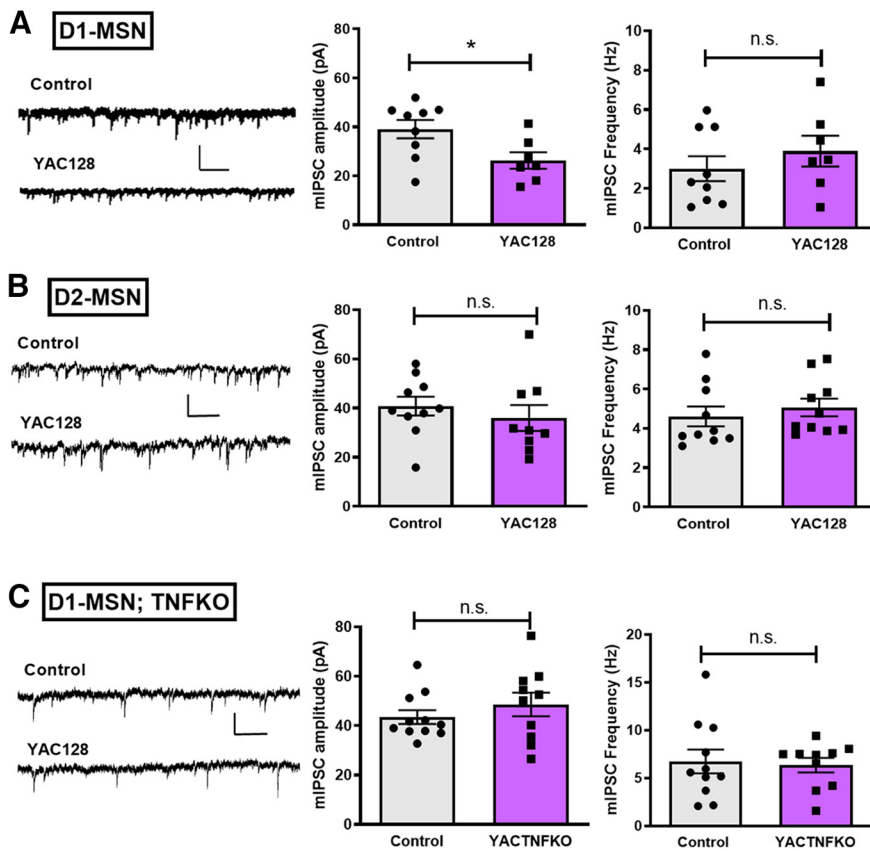
Figure 3. Decreased inhibitory synaptic strength on D1-MSNs in YAC128 mice is also TNF-dependent. *A*, Sample traces and group data of mIPSCs recorded from D1-MSNs. YAC128 mice had a decreased average amplitude of mIPSCs (two-tailed *t* test, $t_{(14)} = 2.466$, $p = 0.0272$) with no change in frequency ($t_{(14)} = 0.9002$, $p = 0.3832$) compared with control littermates. Calibration: 50 pA, 500 ms. *B*, Sample traces and group data of mIPSCs from D2-MSNs. No changes were seen in either amplitude (*t* test, $t_{(17)} = 0.7477$, $p = 0.4649$) or the frequency (*t* test, $t_{(18)} = 0.6729$, $p = 0.5096$) in YAC128 mice compared with control littermates. Calibration: 100 pA, 500 ms. *C*, Sample traces and group data of mIPSCs on D1-MSNs from $TNF^{-/-}$; YAC128 mice. No changes were observed in either amplitude (two-tailed *t* test, $t_{(19)} = 0.9455$, $p = 0.3563$) or frequency (two-tailed *t* test, $t_{(19)} = 0.26$, $p = 0.7977$). Calibration: 100 pA, 500 ms.

needle 3-4 times, gently agitated for 30 min at 4 degrees, spun at $16,000 \times g$, and the supernatant collected. Biotinylated proteins were isolated by incubating lysates with NeutrAvidin agarose resin (Thermo Scientific) for 1 h at 4°C. Biotinylated proteins were eluted with $2\times$ SDS sample buffer and analyzed by SDS-PAGE along with corresponding total lysates, and probed for surface and total GluA1 (Neuromab 75-327) and GAPDH (Millipore MAB374).

Statistical analysis
All data are presented as mean ± SEM. Statistical analyses were performed using JASP software (University of Amsterdam) or GraphPad Prism 6 software. Parametric tests, including two-tailed Student's *t* test, one-way ANOVA, and two-way ANOVA, were performed if the dataset for the experiment was normally distributed. If the dataset did not meet criteria, then an equivalent nonparametric test, the Mann–Whitney *U* test, was used instead. Furthermore, if we could not assume equality of variance in a dataset (tested with the Levene test), we performed a Welch's correction or performed a nonparametric test. *Post hoc* analysis was performed using the Newman-Keuls test.

Results

YAC128 mice have altered glutamatergic synapses on D1-MSNs in the striatum
First, we wanted to determine whether synaptic strength was different in presymptomatic 8- to 12-week-old YAC128 mice. To do so, we recorded AMPA/NMDA ratios on both D1-expressing presumptive direct pathway MSNs (D1-MSNs; expressing tD-Tomato under the D1 promotor) and from D1-nonexpressing presumptive indirect pathway MSNs (D2-MSNs). The brightness of D1-Tomato allow us to be relatively confident the nonfluorescent MSNs are indeed D2-MSNs (Ade et al., 2011).

We observed a significant increase in the AMPA/NMDA ratio on D1-MSNs from YAC128 mice compared with their non–YAC128-expressing littermates (Fig. 1A). However, no changes were observed in AMPA/NMDA ratios on D2-MSNs (Fig. 1B). As changes in extrasynaptic NMDAR have been reported in HD models (Milnerwood et al., 2010), we wanted to determine whether the changes in the AMPA/NMDA ratio were because of changes in the AMPA-mediated current or the NMDA-mediated current. First, we measured the rectification index of the isolated AMPA currents, which reflects the proportion of inwardly rectifying calcium-permeable AMPARs. We compared isolated AMPA currents recorded at +40 and −70 mV, and observed a significant decrease in this ratio on D1-MSNs from YAC128 animals compared with control littermates (Fig. 1C). This would equate to an increase in rectification and suggest an increased percentage of calcium-permeable AMPARs at the synapse. Next, we generated I/O curves of both currents for D1-MSNs from control and YAC128 mice by pharmacologically isolating these currents while varying the stimulation intensity. Isolated AMPA currents were larger for D1-MSNs from YAC128 mice, compared with control cells, across the range of stimulation intensities (Fig. 1D), in contrast to NMDA currents that were unchanged between the genotypes (Fig. 1E). Overall, these data indicate that glutamatergic synaptic strength is increased in YAC128 mice, specifically on D1-MSNs, and this is due at least in part by the insertion of calcium-permeable AMPARs.

The changes in glutamatergic synaptic strength in YAC128 mice are TNF-dependent
Our previous work has shown that the pro-inflammatory cytokine TNF is a potent regulator of glutamatergic synapses (Beattie et al., 2002; Lewitus et al., 2014), in part by changing the trafficking of calcium-permeable AMPARs (Stellwagen et al., 2005; Lewitus et al., 2014); further, in the striatum, this occurs primarily on D1-MSNs (Lewitus et al., 2016). As TNF is elevated in the striatum at later stages in the YAC128 mouse (Soulet and Cicchetti, 2011), we hypothesized that TNF could be driving the observed synaptic changes. We first checked whether TNF was elevated in YAC128 mice at the ages used above (8-12 weeks). Striatal TNF levels were measured by ELISA, which showed a 57% increase of TNF in YAC128 mice compared with control littermates (Fig. 2A). We next investigated if this TNF could contribute the synaptic changes observed. To test this idea, we crossed the

D1-labeled YAC128 mice with $TNF^{-/-}$ mice, comparing YAC128; $TNF^{-/-}$ with $TNF^{-/-}$ littermates. While we observed no basal difference between the AMPA/NMDA ratios of D1-MSNs or D2-MSNs of $TNF^{-/-}$ mice compared with WT mice, the YAC128-induced increase in AMPA/NMDA ratio on D1-MSNs was completely absent when TNF was genetically deleted (Fig. 2B,C). No changes were seen on D2-MSNs, as expected (Fig. 2D). The loss of the YAC128 phenotype in the $TNF^{-/-}$ mice could be because of a developmental issue or it could be because of ongoing TNF signaling in the adult. To test this possibility, we pharmacologically inhibited TNF signaling using a blood–brain barrier permeant DN version of TNF (DN-TNF; 30 mg/kg), injected subcutaneously 48 h before the recordings. This relatively short-term blockade was capable of reversing the change in AMPA/NMDA ratio seen on D1-MSNs, as ratios in YAC128 mice treated with DN-TNF were indistinguishable from DN-TNF-treated control littermates (Fig. 2E). DN-TNF treatment also did not affect ratios on D2-MSNs (Fig. 2F), consistent with what was seen with the $TNF^{-/-}$ mice. Together, these data demonstrate that the changes at glutamatergic synapses in YAC128 mice are driven and maintained by ongoing TNF signaling.

Inhibitory synaptic strength is reduced in a TNF-dependent manner

For hippocampal pyramidal cells, TNF is known to inversely regulate glutamatergic and GABAergic synapses, with acute TNF treatment causing the insertion of AMPARs and the removal of GABA$_A$ receptors (Stellwagen et al., 2005; Pribiag and Stellwagen, 2013). As we saw TNF-dependent changes at glutamate synapses, we wanted to examine the inhibitory currents on MSNs. To do so, we recorded mIPSCs from both D1- and D2-MSNs in presymptomatic YAC128 mice. On D1-MSNs, we observed a significant decrease in mIPSC amplitude, with no change in the frequency, compared with control littermates (Fig. 3A). As with the excitatory synapses, no changes were seen at inhibitory synapses on D2-MSNs (Fig. 3B). As decreased inhibitory synaptic strength combined with increased excitatory synaptic strength would be consistent with TNF-induced synaptic plasticity, we then tested whether the changes on D1-MSNs were TNF-dependent. To do so, we recorded mIPSCs in YAC128; $TNF^{-/-}$ mice and observed no significant differences in either amplitude or frequency, compared with $TNF^{-/-}$ littermates (Fig. 3C). This indicates that there is a TNF-mediated decrease in inhibitory synaptic strength specifically on D1-MSNs in the YAC128 model mouse.

TNF signaling saturated in presymptomatic YAC128 mice

Based on our previous experiments (Lewitus et al., 2014, 2016), we would have expected TNF-mediated synaptic change in the striatum to result in decreased AMPA/NMDA ratios and not the increased ratios observed here. We therefore sought to test whether YAC128 expression fundamental changed the response of striatal neurons to TNF. To test this, we treated striatal slices from YAC128 mice with exogenous TNF, at varying doses for 1 h, and recorded AMPA/NMDA ratios from D1-MSNs. We observed no significant response in YAC128 neurons to TNF in the AMPA/NMDA ratios at 10, 100, or 1000 ng/ml TNF (Fig. 4A). The lack of TNF response (in either direction) may reflect a saturation of TNF signaling because of the elevated TNF seen in the YAC128 mouse (Fig. 2A). To test this hypothesis, we repeated the experiment, but this time using YAC128; $TNF^{-/-}$
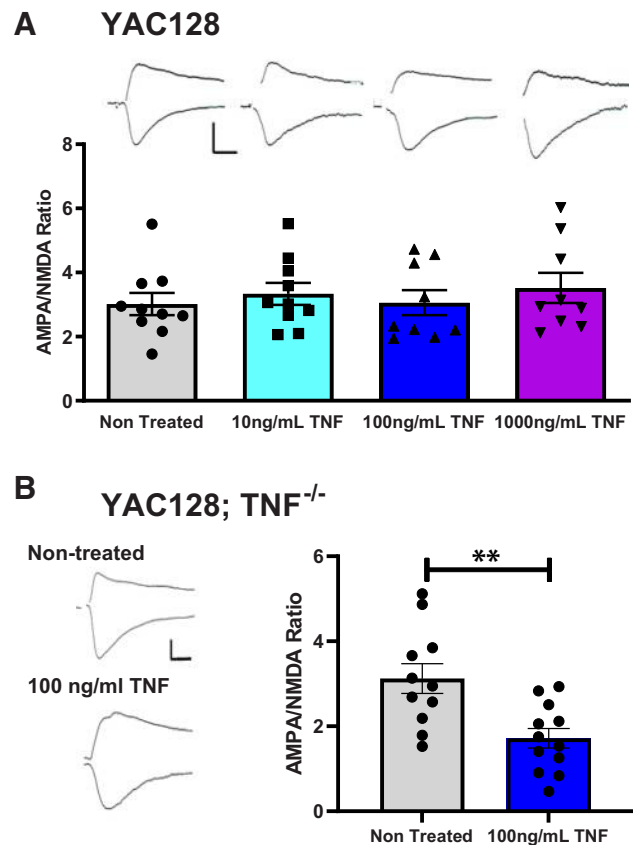

Figure 4. TNF signaling is saturated in presymptomatic YAC128 mice. ***A***, Acute striatal slices from YAC128 mice were treated *ex vivo* with varying concentrations of TNF for 1 h. No significant differences were observed in the AMPA/NMDA ratios on D1-MSNs treated with TNF compared with untreated slices from the same animals (one-way ANOVA, $F_{(3,36)} = 0.4737$, $p = 0.7025$). ***B***, Acute striatal slices from $TNF^{-/-}$; YAC128 mice were treated with 100 ng/ml TNF. There was a significant decrease in the AMPA/NMDA ratio on D1-MSNs from TNF-treated slices compared with untreated slices from the same animals (two-tailed t test, $t_{(21)} = 3.405$, $p = 0.0027$). Calibration: 200 pA, 10 ms.

mice. Here exogenous treatment with 100 ng/ml TNF resulted in decreased AMPA/NMDA ratios (Fig. 4B), similar to what we had observed with acute TNF treatments in control mice (Lewitus et al., 2014, 2016). This indicates that YAC128 expression has not fundamentally changed the D1-MSN response to TNF and suggests instead that the chronic presence of TNF in the YAC128 striatum may cause the AMPA/NMDA ratio to increase rather than decrease, which we see with acute exogenous treatments of TNF.

To test this idea, we then treated acute slices from WT animals with higher levels of TNF. Slices treated with 1000 ng/ml TNF for 30 min had increased AMPA/NMDA ratios on D1-MSNs compared with untreated control slices from the same animals (Fig. 5A), although D2-MSNs remained largely unaffected (Fig. 5B). This effect was still because of activation of TNFR1, as treatment of slices from $TNFR1^{-/-}$ mice did not increase AMPA/NMDA ratios (Fig. 5C), indicating that high-dose TNF did not engage TNFR2. We next verified that the change in AMPA/NMDA ratio was still because of a change in AMPAR surface expression, as we previously demonstrated for the lower dose of TNF (Lewitus et al., 2014). Acute striatal slices were treated with varying doses of TNF and the surface proteins tagged with biotin. Analysis of the surface fraction of AMPARs revealed that 100 ng/ml TNF led to a significant reduction in
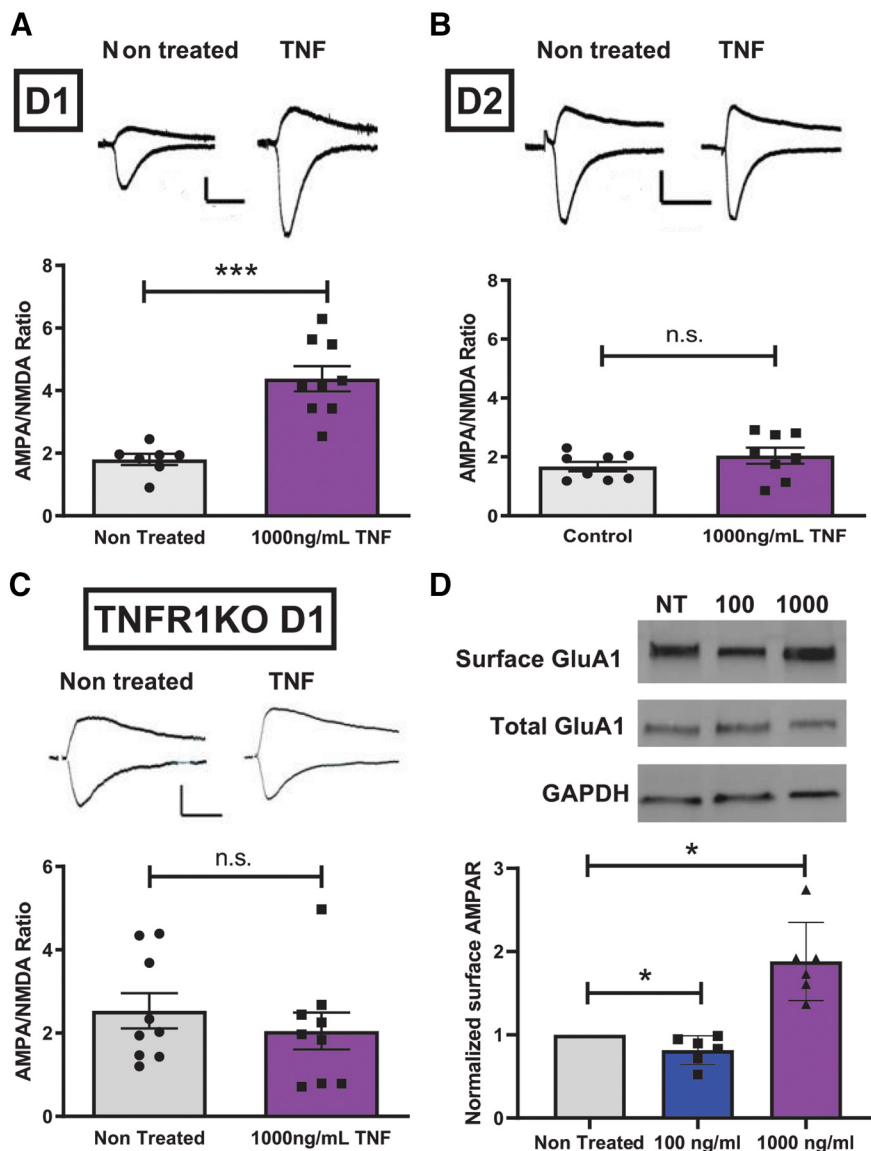
Figure 5. Dose-dependent effects of TNF on striatal glutamatergic synapses. *A*, High-dose TNF treatment (1000 ng/ml; 30 min) of acute striatal slices from WT mice leads to an increase in AMPA/NMDA ratio on D1-MSNs (two-tailed t test with Welch correction, $t_{(10)} = 5.847$, $p = 0.0001$), compared with untreated slices from the same animals. *B*, High-dose TNF treatment did not alter the AMPA/NMDA ratio on D2-MSNs (two-tailed t test, $t_{(14)} = 1.180$, $p = 0.2578$). *C*, High-dose TNF treatment did not significantly change AMPA/NMDA ratios on D1-MSNs from $TNFR1^{-/-}$ mice (two-tailed t test, $t_{(16)} = 0.7960$, $p = 0.4377$). *D*, Sample Western blots and group data for surface biotinylated GluA1 and total GluA1 from striatal slices from WT mice treated with high-dose TNF, showing that treatment increased the surface levels of GluA1 relative to untreated control slices from the same animals (Kruskal–Wallis test, $H_{(3)} = 7.448$, $p = 0.0036$). Calibration: 50pA, 20ms.

a decrease in AMPA/NMDA ratios, we observed an increase in mIPSC amplitude with no change in frequency (Fig. 6*A*,*B*). However, at 1000 ng/ml, where instead there is an increase in AMPA/NMDA ratio, we now observed a decrease in mIPSC amplitude, again with no change in frequency (Fig. 6*A*,*B*). No significant changes were seen in D2-MSNs at either dose of TNF (Fig. 6*C*,*D*). Therefore, the changes in synaptic function in D1-MSNs seen in the HD model mice appear to reflect maximal and ongoing TNF signaling in the striatum.

Discussion

Here we present evidence that both glutamatergic and GABAergic synapses are altered at early presymptomatic stages in the YAC128 HD model mouse. We observed an increase in AMPA/NMDA ratio and a decrease in mIPSC amplitude specifically on D1-MSNs, which was not seen on D2-MSNs. The changes in AMPA/NMDA ratio were likely because of an increase in AMPARs at the synapse, as the AMPA I/O curve was increased while the NMDA I/O was not. Further, we saw a shift in the rectification index of AMPA currents, suggesting the addition of calcium-permeable AMPARs. Both the change at excitatory and at inhibitory synapses were TNF-dependent, as blocking TNF signaling (even for 48 h) was sufficient to restore normal synaptic function at both types of synapses. The HD-related changes were similar to the synaptic changes induced by high dose TNF signaling, suggesting that TNF signaling in the striatum is saturated in this HD disease model.

TNF levels themselves are only modestly elevated in the YAC128 mouse, a bit >50% above baseline values. The literature varies on whether TNF is detectably elevated in this model, particularly at early time points (Soulet and Cicchetti, 2011). However, this chronic elevation is sufficient to induce synaptic changes on D1-MSNs, and therefore is clearly consequen-

surface AMPARs; but in contrast, 1000 ng/ml TNF resulted in a substantial increase in surface AMPARs in the striatum (Fig. 5*D*). This strongly suggests that the observed change in AMPA/NMDA ratio is due a change in AMPAR trafficking for both doses of TNF, and not an involvement of the NMDAR at the higher dose.

We also observed that inhibitory currents had a similar dose-dependent response. Our previous work on hippocampal pyramidal cells had demonstrated that the TNF-mediated response of inhibitory synapses was inverted from the response of glutamatergic synapses, where we saw stronger glutamate synapses and weaker inhibitory ones (Stellwagen et al., 2005). Testing D1-MSNs, the change at inhibitory synapses was again inverted from that of glutamate synapses. At 100 ng/ml, where there is

tial. Further, the changes that occur are akin to the changes induced by maximal acute TNF signaling, suggesting that low chronic levels of TNF lead to an accumulation of signaling. It is interesting that the synaptic response to high levels of TNF is reversed from what we have observed with more moderate acute TNF signaling in the striatum and instead resembles the moderate acute response in hippocampal pyramidal cells (Lewitus et al., 2014). The precise intracellular signaling cascades responsible have not been fully identified, but this reversal may represent the differential targeting, with a kinase (driving receptor exocytosis, as has been shown in hippocampal pyramidal neurons) (Beattie et al., 2002) and phosphatase (driving receptor endocytosis; likely PP1) targeted separately to excitatory and inhibitory synapses.

By reversing the targeting, the neuron could then reverse the synaptic effects of TNF, switching from a decrease in AMPARs and increase in GABA-A receptors to an increase in AMPARs and loss of GABA-A receptors.

The HD-driven TNF signaling in striatum leads to an early change in excitatory–inhibitory balance on D1-MSNs, with an increase in glutamatergic drive and a decrease in inhibitory drive. The change was restricted to D1-MSNs, as we observed little change at either type of synapse for D2-MSNs. Previous work did not observe changes in glutamatergic synaptic properties of MSNs, although changes were observed in extrasynaptic NMDARs (Milnerwood et al., 2010). However, this study did not distinguish between D1-MSNs and D2-MSNs, which would likely obscure the phenotype described here. Indeed, they did see a trend for an increase in AMPA/NMDA ratios on MSNs in the YAC128 mice, although it was not significant. Similarly, if we combine our D1-MSN and D2-MSN datasets using equal numbers of cells of each type, we observe a trend for an increase in AMPA/NMDA ratio in YAC128 MSNs (2.30 ± 0.20 vs 2.77 ± 0.24, $n = 38$ and $n = 28$), but the change is no longer significant ($p = 0.131$). Thus, being able to differentiate D1-MSNs from D2-MSNs is essential to observing a synaptic change that is restricted to D1-MSNs.

At least some of the newly inserted AMPARs are likely GluA2-lacking, calcium-permeable AMPARs, based on the change in rectification. This is consistent with the TNF-mediated AMPAR exocytosis observed in hippocampal neurons (Ogoshi et al., 2005; Stellwagen et al., 2005), and could greatly increase a neuron's potential for excitotoxicity (Ying et al., 1997; Yu et al., 2002; Kwak and Weiss, 2006). Excitotoxicity is a major contributor to the neurodegeneration seen in HD, although much of the focus has been on contribution of NMDARs (Marco et al., 2013; Milnerwood and Raymond, 2010; Milnerwood et al., 2010). In addition, changes in glutamate release or reuptake have also been hypothesized to contribute (Ehrlich, 2012), likely because of astrocyte dysfunction (Lievens et al., 2001). Presymptomatic animals also have increased excitotoxic potential, with larger lesions in response to excitotoxic challenge (Graham et al., 2009), again suggesting stronger synapses. TNF may be a contributor to this increased potential. Indeed, TNF-mediated cell death occurs through this excitotoxic pathway in retinal ganglion cell (Lebrun-Julien et al., 2009), the hippocampus (Leonoudakis et al., 2008), and the spinal cord (Hermann et al., 2001). Thus, the increase in excitatory drive on D1-MSNs, combined with the decrease in inhibitory drive, may contribute to disease progression. However, that D2-MSNs are considered to be the first to degenerate (Raymond et al., 2011), rather than the D1-MSNs, suggests that multiple factors contribute to the neurodegeneration in HD.

Most likely, HD is a complex interaction of cell-autonomous and non–cell-autonomous consequences of mHTT expression (Ehrlich, 2012). Glial cells are the prime producers of cytokines in the CNS, and recent evidence suggests that glia may play a
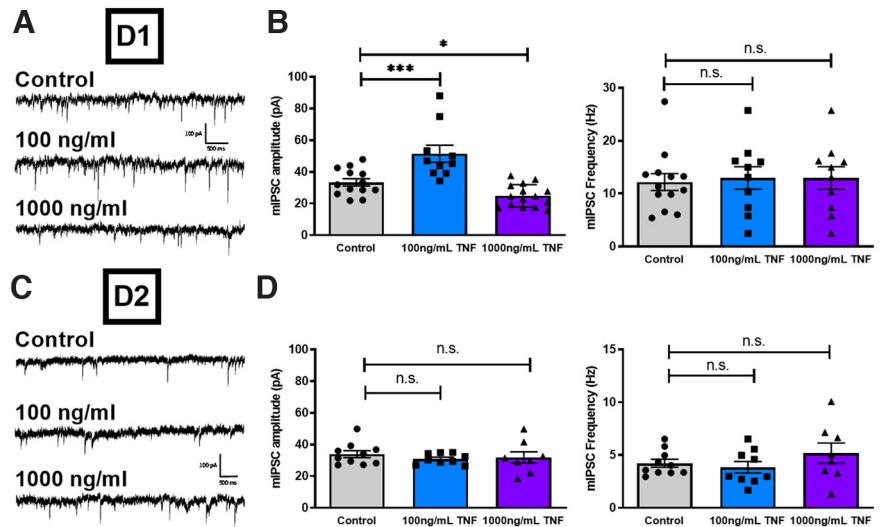

Figure 6. Dose-dependent effects of TNF on striatal inhibitory synaptic strength are reversed from glutamatergic changes. **A**, Sample traces and (**B**) group data showing the dose-dependent TNF changes to mIPSC amplitude on D1-MSNs from WT mice compared with untreated slices from the same animals (one-way ANOVA, $F_{(2,35)} = 18.21$, $p < 0.0001$). TNF treatment did not change the mIPSC frequency on D1-MSNs (one-way ANOVA, $F_{(2,30)} = 0.05,838$, $p = 0.9434$). **C**, Sample traces and (**D**) group data for D2-MSNs. There were no significant changes in the amplitude of mIPSCs on D2-MSNs in response to either dose of TNF (one-way ANOVA, $F_{(2,24)} = 0.4285$, $p = 0.6564$). TNF treatment also did not affect the mIPSC frequency on D2-MSNs (one-way ANOVA, $F_{(2,24)} = 1.120$, $p = 0.3426$).

critical role in disease progression. mHTT is expressed in both microglia and astrocytes (Bjorkqvist et al., 2008; Bradford et al., 2009, 2010), and there are regional differences in the astrocyte response in HD (Vonsattel et al., 1985; Al-Dalahmah et al., 2020). Similar regionality is seen in the microglia activation observed in HD models, and the density of microglia activation correlates with severity of the disease (Sapp et al., 2001). Importantly, glial activation precedes disease onset (Tai et al., 2007; Politis et al., 2011), suggesting that activation is not simply a consequence of the disease. Indeed, astrocyte-only expression of mHTT can cause neurologic impairments (Bradford et al., 2009) and can exacerbate the dysfunctions associated with neuronal expression (Bradford et al., 2010). Similarly, damping microglia activation with CB2 agonists can reduce neurodegeneration (Palazuelos et al., 2009), although minocycline and other microglial modulators have given inconsistent and generally disappointing results (for review, see Soulet and Cicchetti, 2011). Based on the data presented here, TNF is likely one of the glial factors influencing HD onset and progression, but there are probably many such factors that vary over time.

TNF is clearly altering synapses on D1-MSNs in relatively young mice (8-10 weeks). Previous work has found a number of changes on D1-MSNs in HD model mice, including increases in EPSC frequency, mEPSC frequency, and release probability, indicating possible changes in glutamate release probability or overall changes in glutamate synapses (Joshi et al., 2009; Cepeda et al., 2010; Raymond et al., 2011). Here we see evidence for postsynaptic changes, with changes in AMPA/NMDA ratios and mIPSC amplitudes. This suggests that there are changes throughout the glutamate system, as well as to the inhibitory signaling in the striatum. However, it is unclear whether the TNF-dependent changes are part of the disease process or a response to it. TNF is a cytokine that also has a key role in homeostatic synaptic plasticity, helping to restore excitatory–inhibitory balance after prolonged changes in neuronal activity (Stellwagen and Malenka, 2006), and acts to adaptively change striatal synapses during

the development of dyskinesia and addiction-related behaviors (Lewitus et al., 2014, 2016). Thus, TNF signaling in HD could be related to symptom reduction, although the increase in D1-MSN excitability may also increase the potential for excitotoxicity. In addition, TTX-induced homeostatic synaptic plasticity is disrupted in cortical cultures from YAC128 mice (Smith-Dijak et al., 2019), which implies mis-regulation of the glial TNF response. This could imply that the striatal TNF signaling is also mis-regulated and, therefore, part of the disease process and not an adaptive response. Consistent with this idea, infusion of DN-TNF into the R6/2 HD model mice improved motor function, reduced mHTT aggregates, and increased neuronal density (Hsiao et al., 2014). Linking the synaptic changes to changes in striatal function will be necessary to determine the full impact of elevated TNF signaling in HD. It will also be necessary to test the various models of HD, to make sure these are not specific to a model.

We have uncovered the early impact of elevated TNF on striatal MSNs in a mouse model of HD. These early changes may help precipitate later pathologies, including striatal degeneration. The increased CP-AMPAR combined with dysregulated glutamate and GABA signaling may have significant impact on disease progression. These novel findings may help devise appropriate early strategies for HD treatments.

References

Ade K, Wan Y, Chen M, Gloss B, Calakos N (2011) An improved BAC transgenic fluorescent reporter line for sensitive and specific identification of striatonigral medium spiny neurons. Front Syst Neurosci 5:32.

Al-Dalahmah O, Sosunov AA, Shaik A, Ofori K, Liu Y, Vonsattel JP, Adorjan I, Menon V, Goldman JE (2020) Single-nucleus RNA-seq identifies Huntington disease astrocyte states. Acta Neuropathol Commun 8:19.

Alto LT, Chen X, Ruhn KA, Trevino I, Tansey MG (2014) AAV-dominant negative tumor necrosis factor (DN-TNF) gene transfer to the striatum does not rescue medium spiny neurons in the YAC128 mouse model of Huntington's disease. PLoS One 9:e96544.

Bates GP, Dorsey R, Gusella JF, Hayden MR, Kay C, Leavitt BR, Nance M, Ross CA, Scahill RI, Wetzel R, Wild EJ (2015) Huntington disease. Nat Rev Dis Primers 1:15005.

Beattie EC, Stellwagen D, Morishita W, Bresnahan JC, Ha BK, Von Zastrow M, Beattie MS, Malenka RC (2002) Control of synaptic strength by glial TNFalpha. Science 295:2282–2285.

Bjorkqvist M, et al. (2008) A novel pathogenic pathway of immune activation detectable before clinical onset in Huntington's disease. J Exp Med 205:1869–1877.

Bradford J, Shin JY, Roberts M, Wang CE, Li XJ, Li S (2009) Expression of mutant huntingtin in mouse brain astrocytes causes age-dependent neurological symptoms. Proc Natl Acad Sci USA 106:22480–22485.

Bradford J, Shin JY, Roberts M, Wang CE, Sheng G, Li S, Li XJ (2010) Mutant huntingtin in glial cells exacerbates neurological symptoms of Huntington disease mice. J Biol Chem 285:10653–10661.

Caramins M, Halliday G, McCusker E, Trent RJ (2003) Genetically confirmed clinical Huntington's disease with no observable cell loss. J Neurol Neurosurg Psychiatry 74:968–970.

Cepeda C, Cummings DM, Andre VM, Holley SM, Levine MS (2010) Genetic mouse models of Huntington's disease: focus on electrophysiological mechanisms. ASN Neuro 2:e00033.

Ehrlich ME (2012) Huntington's disease and the striatal medium spiny neuron: cell-autonomous and non–cell-autonomous mechanisms of disease. Neurotherapeutics 9:270–284.

Goodliffe JW, Song H, Rubakovic A, Chang W, Medalla M, Weaver CM, Luebke JI (2018) Differential changes to D1 and D2 medium spiny neurons in the 12-month-old Q175$^{+/-}$ mouse model of Huntington's disease. PLoS One 13:e0200626.

Graham RK, Pouladi MA, Joshi P, Lu G, Deng Y, Wu NP, Figueroa BE, Metzler M, Andre VM, Slow EJ, Raymond L, Friedlander R, Levine MS, Leavitt BR, Hayden MR (2009) Differential susceptibility to excitotoxic

stress in YAC128 mouse models of Huntington disease between initiation and progression of disease. J Neurosci 29:2193–2204.

Heir R, Stellwagen D (2020) TNF-mediated homeostatic synaptic plasticity: from in vitro to in vivo models. Front Cell Neurosci 14:565841.

Hermann GE, Rogers RC, Bresnahan JC, Beattie MS (2001) Tumor necrosis factor-alpha induces cFOS and strongly potentiates glutamate-mediated cell death in the rat spinal cord. Neurobiol Dis 8:590–599.

Hodgson JG, Agopyan N, Gutekunst CA, Leavitt BR, LePiane F, Singaraja R, Smith DJ, Bissada N, McCutcheon K, Nasir J, Jamot L, Li XJ, Stevens ME, Rosemond E, Roder JC, Phillips AG, Rubin EM, Hersch SM, Hayden MR (1999) A YAC mouse model for Huntington's disease with full-length mutant huntingtin, cytoplasmic toxicity, and selective striatal neurodegeneration. Neuron 23:181–192.

Hsiao HY, Chiu FL, Chen CM, Wu YR, Chen HM, Chen YC, Kuo HC, Chern Y (2014) Inhibition of soluble tumor necrosis factor is therapeutic in Huntington's disease. Hum Mol Genet 23:4328–4344.

Joshi PR, Wu NP, Andre VM, Cummings DM, Cepeda C, Joyce JA, Carroll JB, Leavitt BR, Hayden MR, Levine MS, Bamford NS (2009) Age-dependent alterations of corticostriatal activity in the YAC128 mouse model of Huntington disease. J Neurosci 29:2414–2427.

Kwak S, Weiss JH (2006) Calcium-permeable AMPA channels in neurodegenerative disease and ischemia. Curr Opin Neurobiol 16:281–287.

Lanciego JL, Luquin N, Obeso JA (2012) Functional neuroanatomy of the basal ganglia. Cold Spring Harb Perspect Med 2:a009621.

Lebouc M, Richard Q, Garret M, Baufreton J (2020) Striatal circuit development and its alterations in Huntington's disease. Neurobiol Dis 145:105076.

Lebrun-Julien F, Duplan L, Pernet V, Osswald I, Sapieha P, Bourgeois P, Dickson K, Bowie D, Barker PA, Di Polo A (2009) Excitotoxic death of retinal neurons in vivo occurs via a non–cell-autonomous mechanism. J Neurosci 29:5536–5545.

Leonoudakis D, Zhao P, Beattie EC (2008) Rapid tumor necrosis factor alpha-induced exocytosis of glutamate receptor 2-lacking AMPA receptors to extrasynaptic plasma membrane potentiates excitotoxicity. J Neurosci 28:2119–2130.

Lewitus GM, Konefal SC, Greenhalgh AD, Pribiag H, Augereau K, Stellwagen D (2016) Microglial TNF-alpha suppresses cocaine-induced plasticity and behavioral sensitization. Neuron 90:483–491.

Lewitus GM, Pribiag H, Duseja R, St-Hilaire M, Stellwagen D (2014) An adaptive role of TNFalpha in the regulation of striatal synapses. J Neurosci 34:6146–6155.

Lievens JC, Woodman B, Mahal A, Spasic-Boscovic O, Samuel D, Kerkerian-Le Goff L, Bates GP (2001) Impaired glutamate uptake in the R6 Huntington's disease transgenic mice. Neurobiol Dis 8:807–821.

Marco S, Giralt A, Petrovic MM, Pouladi MA, Martinez-Turrillas R, Martinez-Hernandez J, Kaltenbach LS, Torres-Peraza J, Graham RK, Watanabe M, Luján R, Nakanishi N, Lipton SA, Lo DC, Hayden MR, Alberch J, Wesseling JF, Pérez-Otaño I (2013) Suppressing aberrant GluN3A expression rescues synaptic and behavioral impairments in Huntington's disease models. Nat Med 19:1030–1038.

Menalled L, El-Khodor BF, Patry M, Suarez-Farinas M, Orenstein SJ, Zahasky B, Leahy C, Wheeler V, Yang XW, McDonald M, Morton AJ, Bates G, Leeds J, Park L, Howland D, Signer E, Tobin A, Brunner D (2009) Systematic behavioral evaluation of Huntington's disease transgenic and knock-in mouse models. Neurobiol Dis 35:319–336.

Milnerwood AJ, Raymond LA (2010) Early synaptic pathophysiology in neurodegeneration: insights from Huntington's disease. Trends Neurosci 33:513–523.

Milnerwood AJ, Gladding CM, Pouladi MA, Kaufman AM, Hines RM, Boyd JD, Ko RW, Vasuta OC, Graham RK, Hayden MR, Murphy TH, Raymond LA (2010) Early increase in extrasynaptic NMDA receptor signaling and expression contributes to phenotype onset in Huntington's disease mice. Neuron 65:178–190.

Ogoshi F, Yin HZ, Kuppumbatti Y, Song B, Amindari S, Weiss JH (2005) Tumor necrosis-factor-alpha (TNF-alpha) induces rapid insertion of Ca^{2+}-permeable alpha-amino-3-hydroxyl-5-methyl-4-isoxazole-propionate (AMPA)/kainate (Ca-A/K) channels in a subset of hippocampal pyramidal neurons. Exp Neurol 193:384–393.

Palazuelos J, Aguado T, Pazos MR, Julien B, Carrasco C, Resel E, Sagredo O, Benito C, Romero J, Azcoitia I, Fernández-Ruiz J, Guzmán M, Galve-Roperh I (2009) Microglial CB2 cannabinoid receptors are neuroprotective in Huntington's disease excitotoxicity. Brain 132:3152–3164.

Politis M, Pavese N, Tai YF, Kiferle L, Mason SL, Brooks DJ, Tabrizi SJ, Barker RA, Piccini P (2011) Microglial activation in regions related to cognitive function predicts disease onset in Huntington's disease: a multimodal imaging study. Hum Brain Mapp 32:258–270.

Pouladi MA, Morton AJ, Hayden MR (2013) Choosing an animal model for the study of Huntington's disease. Nat Rev Neurosci 14:708–721.

Pribiag H, Stellwagen D (2013) TNF-alpha downregulates inhibitory neurotransmission through protein phosphatase 1-dependent trafficking of GABA(A) receptors. J Neurosci 33:15879–15893.

Raymond LA, Andre VM, Cepeda C, Gladding CM, Milnerwood AJ, Levine MS (2011) Pathophysiology of Huntington's disease: time-dependent alterations in synaptic and receptor function. Neuroscience 198:252–273.

Sapp E, Kegel KB, Aronin N, Hashikawa T, Uchiyama Y, Tohyama K, Bhide PG, Vonsattel JP, DiFiglia M (2001) Early and progressive accumulation of reactive microglia in the Huntington disease brain. J Neuropathol Exp Neurol 60:161–172.

Slow EJ, van Raamsdonk J, Rogers D, Coleman SH, Graham RK, Deng Y, Oh R, Bissada N, Hossain SM, Yang YZ, Li XL, Simpson EM, Gutekunst CA, Leavitt BR, Hayden MR (2003) Selective striatal neuronal loss in a YAC128 mouse model of Huntington disease. Hum Mol Genet 12:1555–1567.

Smith-Dijak AI, Nassrallah WB, Zhang LY, Geva M, Hayden MR, Raymond LA (2019) Impairment and restoration of homeostatic plasticity in cultured cortical neurons from a mouse model of Huntington disease. Front Cell Neurosci 13:209.

Soulet D, Cicchetti F (2011) The role of immunity in Huntington's disease. Mol Psychiatry 16:889–902.

Stellwagen D, Beattie EC, Seo JY, Malenka RC (2005) Differential regulation of AMPA receptor and GABA receptor trafficking by tumor necrosis factor-alpha. J Neurosci 25:3219–3228.

Stellwagen D, Malenka RC (2006) Synaptic scaling mediated by glial TNF-alpha. Nature 440:1054–1059.

Tai YF, Pavese N, Gerhard A, Tabrizi SJ, Barker RA, Brooks DJ, Piccini P (2007) Microglial activation in presymptomatic Huntington's disease gene carriers. Brain 130:1759–1766.

Tereshchenko AV, Schultz JL, Bruss JE, Magnotta VA, Epping EA, Nopoulos PC (2020) Abnormal development of cerebellar-striatal circuitry in Huntington disease. Neurology 94:e1908–e1915.

Turmaine M, Raza A, Mahal A, Mangiarini L, Bates GP, Davies SW (2000) Nonapoptotic neurodegeneration in a transgenic mouse model of Huntington's disease. Proc Natl Acad Sci USA 97:8093–8097.

Twelvetrees AE, Yuen EY, Arancibia-Carcamo IL, MacAskill AF, Rostaing P, Lumb MJ, Humbert S, Triller A, Saudou F, Yan Z, Kittler JF (2010) Delivery of GABAARs to synapses is mediated by HAP1-KIF5 and disrupted by mutant huntingtin. Neuron 65:53–65.

van der Plas E, Langbehn DR, Conrad AL, Koscik TR, Tereshchenko A, Epping EA, Magnotta VA, Nopoulos PC (2019) Abnormal brain development in child and adolescent carriers of mutant huntingtin. Neurology 93:e1021–e1030.

Vonsattel JP, Myers RH, Stevens TJ, Ferrante RJ, Bird ED, Richardson EP Jr (1985) Neuropathological classification of Huntington's disease. J Neuropathol Exp Neurol 44:559–577.

Ying HS, Weishaupt JH, Grabb M, Canzoniero LM, Sensi SL, Sheline CT, Monyer H, Choi DW (1997) Sublethal oxygen-glucose deprivation alters hippocampal neuronal AMPA receptor expression and vulnerability to kainate-induced death. J Neurosci 17:9536–9544.

Yu Z, Cheng G, Wen X, Wu GD, Lee WT, Pleasure D (2002) Tumor necrosis factor alpha increases neuronal vulnerability to excitotoxic necrosis by inducing expression of the AMPA-glutamate receptor subunit GluR1 via an acid sphingomyelinase- and NF-kappaB-dependent mechanism. Neurobiol Dis 11:199–213.